Am J Transl Res 2019;11(1):418-429
www.ajtr.org /ISSN:1943-8141/AJTR0082343

Original Article

p38 MAPK signaling is a key mediator for low-intensity pulsed ultrasound (LIPUS) in cultured human omental adipose-derived mesenchymal stem cells

Yaqing Wang[1*], Li Jiang[1*], Tianhua Xu[1], Zhongping Su[1], Xiasheng Guo[2], Juan Tu[2], Dong Zhang[2], Wei Sun[1], Xiangqing Kong[1]

[1]Department of Cardiology, The First Affiliated Hospital of Nanjing Medical University, Nanjing 210029, Jiangsu, PR China; [2]Key Laboratory of Modern Acoustics, Department of Physics, Collaborative Innovation Center of Advanced Microstructure, Nanjing University, Nanjing 210093, Jiangsu, PR China. [*]Equal contributors.

Received July 9, 2018; Accepted December 18, 2018; Epub January 15, 2019; Published January 30, 2019

Abstract: Visceral obesity is an independent risk factor for cardiovascular disorders and lacks effective, non-drug based clinical therapy. The use of low-intensity pulsed ultrasound (LIPUS) to treat chronic pain and bone fracture is well-known, but its application for visceral obesity treatment has not been studied. Here, we evaluated the therapeutic potential of LIPUS by studying its effects, at varying doses, on human omental adipose-derived mesenchymal stem cells (hAMSCs). LIPUS stimulation was applied for 1 min at intensities between 70 and 210 mW/cm^2. Cell viability was measured using the Cell Counting Kit-8 assay. Cell apoptosis was quantified by flow cytometry and immunoblotting of apoptosis marker proteins. We found that a high dose of LIPUS (210 mW/cm^2) promoted apoptosis in hAMSCs, while a low dose (70 mW/cm^2) increased hAMSC viability. Phosphorylation of p38, a mitogen-activated protein kinase (MAPK), increased with high dose LIPUS treatment, but markedly decreased with a low dose. Inhibition of p38 phosphorylation by SB203580, an inhibitor of p38 MAPK activity, rescued the apoptotic effects of high dose LIPUS. Our results showed the dose-dependent, opposing effects of LIPUS on hAMSCs and suggested that p38 plays a key role in mediating the effects of LIPUS on hAMSCs.

Keywords: LIPUS, apoptosis, cell viability, p38 MAPK, human omental adipose-derived mesenchymal stem cells

Introduction

Obesity is a risk factor for medical conditions such as diabetes mellitus, respiratory disorders, osteoarthritis, cancer, chronic kidney disease, and cardiovascular disease [1-3]. It is a growing health threat worldwide. Although body mass index (BMI) levels are widely used as a general guide to evaluate obesity, several studies have reported that waist circumference is a better predictor of risks associated with obesity [4, 5] because it indicates abdominal fat levels. The accumulation of visceral fat (fat surrounding internal organs) is more dangerous than subcutaneous fat (thin layer of fat under the skin and all around the body) [6]. Obesity therapy mainly includes rigorous lifestyle modifications, pharmacotherapy, use of medical devices, and bariatric surgery [7]. Omentectomy (surgical removal of the omentum, which is a thin layer of fatty tissue surrounding the stomach, large intestine, and other abdominal organs) prevents metabolic syndrome in obese rats [8]. Our unpublished data showed that women who underwent omentectomy had lower systemic blood pressure after the procedure.

Low-intensity pulsed ultrasound (LIPUS) is characterized by ultrasound intensities less than 5 W/cm^2. This technique has been used for medical therapy since the 1950s [9]. LIPUS enhances the healing of bone fractures and chronic fracture nonunions [10-12]. It has been suggested that cells translate the mechanical signal of LIPUS in tissues to a biochemical response in bone via integrin-mediated mechano-receptors. This leads to the production of cyclo-oxygenase 2, which stimulates fracture repair [11]. LIPUS also facilitates soft-tissue healing by promoting cell proliferation [12].

LIPUS has shown promise for promoting cell apoptosis of hepatocellular carcinoma cells (ultrasound intensity: 500 mW/cm^2) [13] and osteoclasts (ultrasound intensity: 30 mW/cm^2) [14]. LIPUS has also been reported to inhibit proliferation of osteosarcoma cells (ultrasound intensity: 30 mW/cm^2) [15]. Cong et al. showed that LIPUS (27.37 mW/cm^2) promotes Schwann cell viability and proliferation [16]. A similar dose of LIPUS (30 mW/cm^2) enhances migration and proliferation of MG63s cells [17]. It is interesting that despite variable effects, most of these studies reported a similar dose of LIPUS.

Several studies have also reported that LIPUS influences differentiation of adipose-derived stem cells [18-20]. We inferred that LIPUS could also affect adipose cell function and help treat obesity. Indeed, the beneficial effects of exercise on obesity are enhanced by LIPUS [21]. However, the efficacy and mechanism of LIPUS-mediated therapy for obesity remain unknown. Our previous study showed that a specific dose of LIPUS (109.44 mW/cm^2) inhibits rat visceral preadipocyte proliferation and promotes apoptosis via the p38 pathway [22]. In this study, we showed that different LIPUS intensities differentially affected human omental adipose-derived mesenchymal stem cells (hAMSCs). Specifically, a high intensity of LIPUS (210 mW/cm^2) promoted apoptosis in hAMSCs via the mitogen-activated protein kinase (MAPK) pathway, while a low intensity (70 mW/cm^2) increased cell viability but did not affect proliferation of hAMSCs.

Materials and methods

Human omental adipose-derived mesenchymal stem cell isolation and culture

Omental adipose tissue was obtained from men (BMI > 25 kg/m^2) who underwent radical gastrectomy for gastric cancer. This study was approved by the Ethical Committee of the First Affiliated Hospital of Nanjing Medical University and written informed consent was obtained from each patient. hAMSCs were isolated by collagenase digestion as described previously [23] and cultured in mesenchymal stem cell medium (MSCM; Cat. 7501, ScienCell). Normal cells from passages 3-5 were used for future experiments.

Low-intensity ultrasound stimulation

The LIPUS apparatus consisted of an ultrasonic generator (Verasonics, Inc., USA), a wideband power amplifier (Verasonics, Inc), a planar transducer (0.5 MHz; Haifu, China), and a degassing pump to obtain de-aerated water. The ultrasound transmitter included a signal generator (33250A, Agilent Technologies, Santa Clara, CA, USA), a broadband power amplifier, and a transducer. The receiving end consisted of a needle-shaped hydrophone (HNA-0400, ONDA, Sunnyvale, CA, USA) with an effective diameter of 0.4 mm to measure the acoustic pressure amplitude. The 3D motion system, which was controlled by LabVIEW software (controller model: XPS-C8, Newport, Irvine, CA, USA), scanned the acoustic field distribution of the XY plane. The collected data were digitized and denoised by a digital oscilloscope. Finally, the data were processed using Matlab to generate an acoustic field distribution. A 6-cm dish, seeded with 1 × 10^6 cells, was placed on top of the transducer with de-aerated water in between. LIPUS stimulation was applied for 1 min at a frequency of 0.5 MHz and a voltage of 44 V in 10-ms pulse bursts. The number of cycles was 1,000-3,000. The acoustic pressure in the 6-cm dish was measured (Supplementary Figure 1). A temperature test paper (TMCHallcrest, USA) was adhered to the inner surface of a 6-cm dish to test the temperature. The temperature of the cell culture media in the dishes was maintained below 37°C during the ultrasound procedures (Supplementary Table 1).

CCK-8 assay

Cell viability was determined using a Cell Counting Kit-8 (CCK-8; Dojindo, Japan) according to the manufacturer's protocol. LIPUS-treated hAMSCs and untreated control cells were seeded at a density of 8 × 10^3 cells/well in 96-well plates and cultured in MSCM (Cat. 7501, ScienCell) for 24 h at 37°C in a CO_2 incubator. The culture medium was replaced with Dulbecco's Modified Eagle Medium/Nutrient mixture F12 (DMEM/F12) and incubated for another 24 h. Cells were then cultured in 100 µl of fresh DMEM/F12 supplemented with 10 µl of CCK-8 solution and incubated for an additional 4 h at 37°C. Absorbance at 450 nm was measured using a Synergy™ 2 Microplate Reader (BioTek, USA).

Flow cytometry

LIPUS-treated hAMSCs and control cells were seeded in 12-well plates at a density of 4×10^5 cells/well and then harvested after 24 h. The cells were then incubated with phycoerythrin (PE)-conjugated propidium iodide (PI) and allophycocyanin (APC)-conjugated Annexin-V (Fcmacs Biotech Co. Ltd., China) in binding buffer for 15 min at room temperature, according to the manufacturer's instructions. Cells were washed and sorted using a FACS-Calibur (BD Biosciences, Germany) within 1 h of staining. To test the role of the p38 pathway in LIPUS-induced cell apoptosis, ultrasound-stimulated hAMSCs were treated with the p38 MAPK inhibitor SB203580 (2 mM/per well), for 24 h and then the extent of cell apoptosis was assayed as above.

TUNEL assay

TUNEL staining was performed to observe DNA fragmentation. Briefly, LIPUS-treated hAMSCs (1.5×10^5 cells/well) were plated in 24-well plates. After 24 h, the TUNEL assay (Cat. 12156792910, Roche) was performed and the percentage of TUNEL-positive cells in a viewing field was quantified. At least five viewing fields containing at least 150 cells each were quantified under 20X magnification to obtain each data point.

Real-time analysis of cell growth

LIPUS-treated and control hAMSCs were plated in 16-well E-plates at a concentration of 2×10^3 cells/well and impedance-based growth was monitored continuously for 48 h using the xCELLigence RTCA TP System (ACEA Biosciences Inc., USA).

EdU (5-Ethynyl-2'-deoxyuridine) cell proliferation assay

After LIPUS treatment, the EdU assay (Ribobio) was used to measure cell proliferation according to manufacturer's instructions. Cells were labeled with EdU (10 μmol/L) for 12 h. After fixation in 4% paraformaldehyde for 30 min, cells were permeabilized in 0.5% Triton X-100 for 15 min. Next, the cells were incubated with Apollo® reaction solution and then nuclei were stained with Hoechst33342. After rinsing three times, cells were observed using an inverted fluorescence microscope (Zeiss) with five random fields of view.

Western blot

The hAMSCs were lysed and centrifuged for extraction of whole cell proteins. For western blotting, 30 ng of total protein per sample was loaded in each lane and separated by sodium dodecyl sulphate polyacrylamide gel electrophoresis (SDS-PAGE; gel percentage of 10-15%), transferred onto polyvinylidene difluoride membranes (PVDF; Millipore, USA) and blocked with bovine serum albumin. Membranes were incubated with primary antibodies against total p38 (1:1,000; Cat. 8690, Cell Signaling Technology, USA), phosphorylated p38 (p-p38; 1:1,000; Cat. 4511, Cell Signaling Technology), total extracellular signal-regulated kinase (ERK; 1:1,000; Cat. 4695, Cell Signaling Technology), phosphorylated ERK (p-ERK; 1:1,000; Cat. 4370, Cell Signaling Technology), total c-Jun N-terminal kinase (JNK; 1:1,000; Cat. 9252, Cell Signaling Technology), phosphorylated JNK (p-JNK; 1:1,000; Cat. 4668, Cell Signaling Technology), B-cell lymphoma 2 (Bcl2; 1:1,000; Cat. 2876, Cell Signaling Technology), Bcl-2 associated X (Bax; 1:1,000; Cat. 2772, Cell Signaling Technology), cleaved caspase-3 (CC3; 1:1,000; Cat. 9661, Cell Signaling Technology), phosphorylated eIF2α (p-eIF2α; 1:1,000; Cat. 3597, Cell Signaling Technology), activating transcription factor 4 (ATF-4; 1:1,000; Cat. 11815, Cell Signaling Technology), phosphorylated transforming growth factor beta-activated kinase 1 (p-TAK1; 1:1,000; Cat. 9339, Cell Signaling Technology), and total TAK1 (1:1,000; Cat. 5206, Cell Signaling Technology) at 4°C overnight. The following day, membranes were incubated with secondary antibodies and then developed using an enhanced chemiluminescence (ECL) reagent (ThermoFisher). Blots were scanned on a ChemiDoc MP imager (Bio-Rad) and protein levels were quantified by Image J software. Original western images for all relevant western blots were presented in Supplementary Figures 2 and 3.

Statistical analysis

All data were expressed as the mean ± standard error of the mean (SEM) of three independent experiments. Treatment group values were compared with control values using GraphPad Prism 6.0 software. The Student's

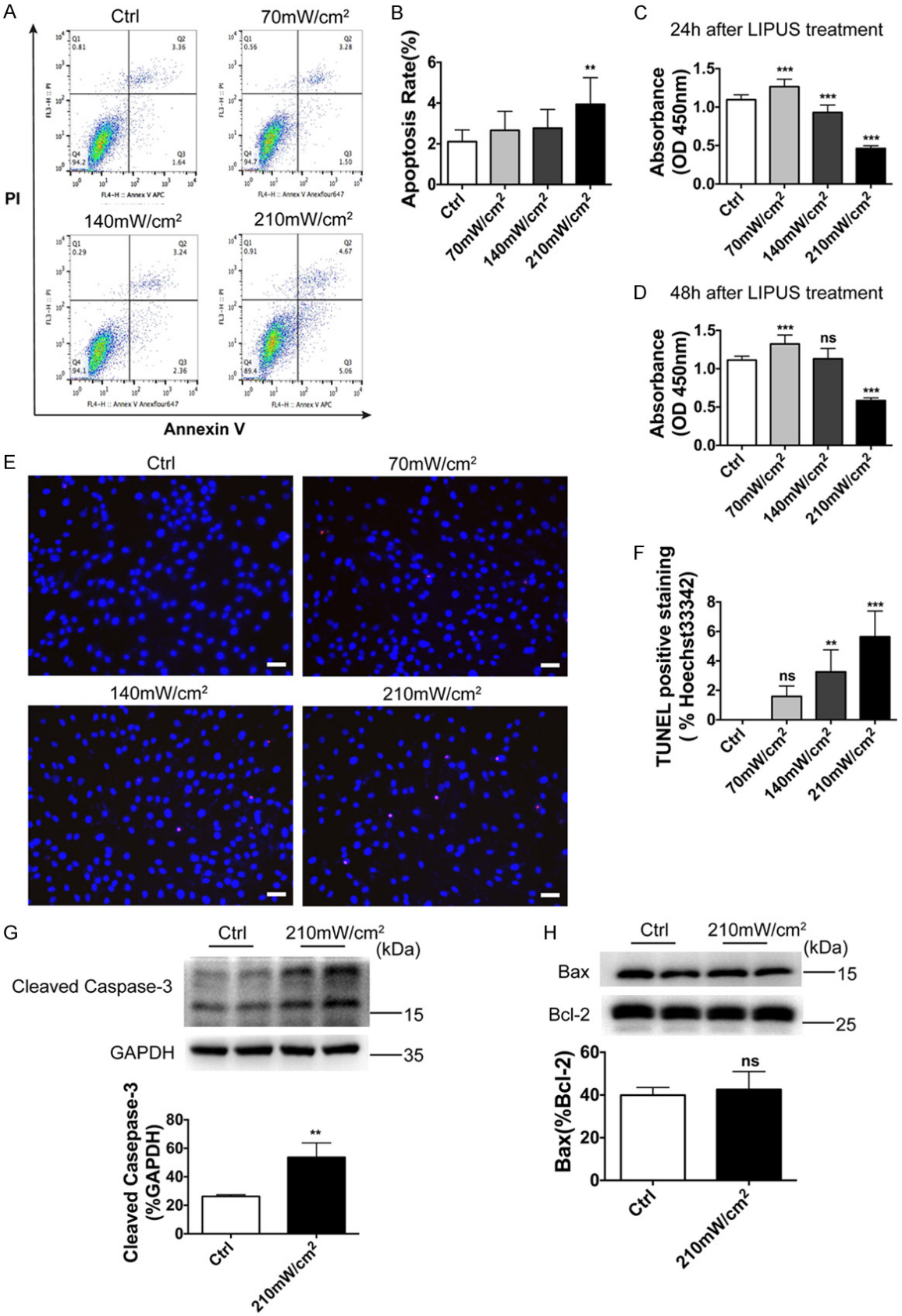
A
Ctrl
70mW/cm²
140mW/cm²
210mW/cm²
PI
Annexin V
B
Apoptosis Rate(%)
Ctrl
70mW/cm²
140mW/cm²
210mW/cm²
C
24h after LIPUS treatment
Absorbance (OD 450nm)
D
48h after LIPUS treatment
ns
E
F
TUNEL positive staining (% Hoechst33342)
G
Cleaved Caspase-3
GAPDH
(kDa)
Cleaved Casepase-3 (%GAPDH)
H
Bax
Bcl-2
Bax(%Bcl-2)

Figure 1. LIPUS promotes apoptosis in hAMSCs. A. Flow cytometric analysis of apoptosis in hAMSCs. Different doses of ultrasound intensities (70, 140, 210 mW/cm^2) were applied. The lower right quadrant shows early apoptotic cells. B. Apoptosis rate of hAMSCs at 24 h post-LIPUS treatment. Data are mean ± SEM. $^{**}P < 0.01$ versus control, one-way ANOVA. C. CCK-8 analysis of hAMSC cell viability at different ultrasound intensities (70, 140, 210 mW/cm^2) 24 h after LIPUS treatment. Data are mean ± SEM. $^{***}P < 0.001$ versus control, one-way ANOVA. D. CCK-8 analysis of hAMSC cell viability at different ultrasound intensities (70, 140, 210 mW/cm^2) 48 h after LIPUS treatment. Data are mean ± SEM. ns $P > 0.05$, $^{***}P < 0.001$ versus control, one-way ANOVA. E. Apoptosis rate was quantified by the TUNEL assay. Scale bar = 50 μm. F. Quantification of TUNEL staining showed that 140 and 210 mW/cm^2 LIPUS doses increased the number of TUNEL-positive cells (apoptosis) compared with control treatment. Data are mean ± SEM. ns $P > 0.05$, $^{**}P < 0.01$, $^{***}P < 0.001$ versus control, one-way ANOVA. G. Western blot analysis of cleaved caspase-3 and GAPDH expression in hAMSCs treated with an ultrasound intensity of 210 mW/cm^2. Cleaved caspase-3 levels were quantified relative to GAPDH levels. Data are mean ± SEM. $^{**}P < 0.01$ versus control, unpaired t-test. H. Western blot analysis of Bax and Bcl-2 expression in hAMSCs treated with an ultrasound intensity of 210 mW/cm^2. Bax/Bcl-2 ratio was calculated. Data are mean ± SEM. $^{**}P < 0.01$ versus control, unpaired t-test.

t-test was used to independently determine statistical differences between two groups. One-way analysis of variance (ANOVA) and Bonferroni's multiple comparison tests were used to compare three groups. *P*-values < 0.05 were considered significant.

Results

High dose of LIPUS promotes apoptosis in hAMSCs

Our previous study showed that a specific dose of LIPUS induces p38-mediated apoptosis in rat visceral pre-adipocytes [15]. To determine the minimum dose of LIPUS that induces apoptosis in hAMSCs, we tested different doses of ultrasound stimulation, with varying power and intensity, on suspensions of hAMSCs (Supplementary Table 1 and Supplementary Figure 1). An increase in cell apoptosis rate was observed at an ultrasound intensity of 210 mW/cm^2 (**Figure 1A** and **1B**). The CCK-8 assay also showed a marked decrease in cell viability at this ultrasound intensity, suggesting that this high dose of LIPUS prevented growth of hAMSCs (**Figure 1C** and **1D**). The proapoptotic effects of LIPUS on hAMSCs were also assessed by the TUNEL assay. The total number of cells were visualized by Hoechest staining and apoptotic cells were visualized by TUNEL staining (**Figure 1E** and **1F**). Ultrasound intensities as low as 140 mW/cm^2 promoted apoptosis compared to the control treatment. Caspase-3 is a protein responsible for proteolysis during apoptosis, and the detection of its cleaved form, CC3, is a reliable marker for cells that undergoing apoptosis [24]. Immunoblotting analysis of CC3 expression confirmed the increase in hAMSCs apoptosis after LIPUS treatment (210 mW/cm^2 intensity; **Figure 1G**). Bcl-2 and Bax belong to the Bcl-2 family of proteins that regulate mitochondrion-mediated apoptotic cell death. The ratio of Bax/Bcl-2 is a measure of a cell's susceptibility to apoptosis [24]. Our results showed that levels of Bax were slightly increased in cells treated with LIPUS at an intensity of 210 mW/cm^2 compared with untreated control cells (**Figure 1H**). No significant differences in the ratio of Bax/Bcl-2 were found between LIPUS-treated and control cells (**Figure 1H**). We also measured the temperature following 70-210 mW/cm^2 doses of LIPUS and found that at the 70 mW/cm^2 dose, the temperature reached 30°C, while doses of 140 and 210 mW/cm^2 increased the temperature to 35°C (Supplementary Table 1).

Low dose of LIPUS enhances viability of hAMSCs, but does not affect cell proliferation

It has been shown that lower doses of LIPUS considerably enhance fracture healing compared with high doses [11]. Therefore, we tested how different doses of LIPUS affected the viability and proliferation of hAMSCs. The cells were stimulated with ultrasound intensities ranging from 70-210 mW/cm^2 and then cultured for 24 h. Cell viability was compared between the differently treatments. We found that cells treated with an ultrasound intensity of 70 mW/cm^2 showed significantly enhanced cell viability compared with the control cells (**Figure 1C**). Cell viability decreased in a dose-dependent manner in cells treated with LIPUS intensities of 140 and 210 mW/cm^2 (**Figure 1C**). We then tested whether the low dose treatment of LIPUS promoted cell proliferation in addition to cell viability in hAMSCs. CCK-8 assays were performed on hAMSCs that were grown in serum-deprived medium to synchronize cell division. No differences in viability were seen between control cells and cells treated with a LIPUS intensity of 140 mW/cm^2

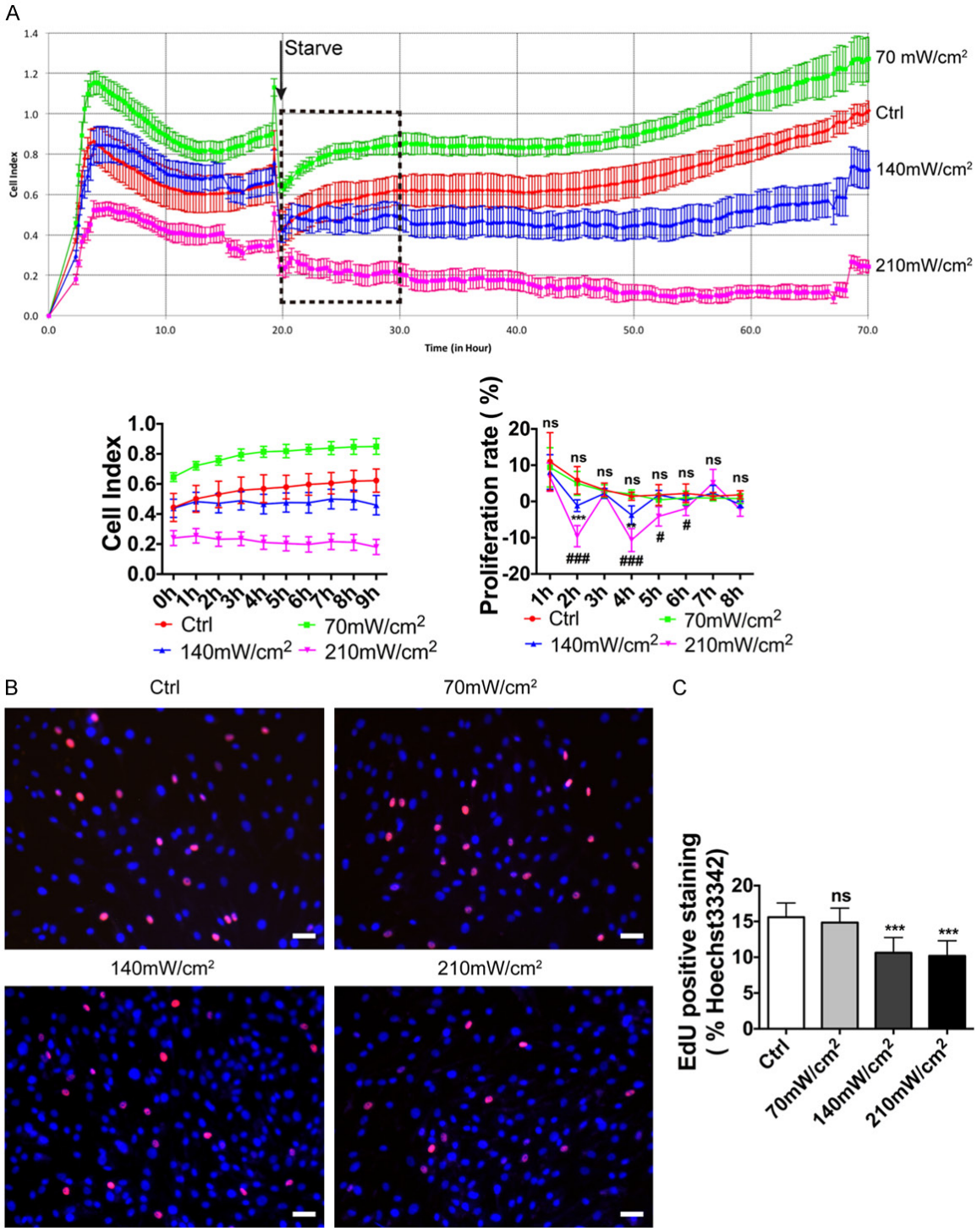

Figure 2. LIPUS does not affect proliferation. A. RTCA analysis of hAMSC proliferation at different ultrasonic doses (70, 140, 210 mW/cm^2). Cell Index was plotted for cells that were starved for 9 h in serum-free medium. Proliferation rate was quantified. Data are mean ± SEM. ns $P > 0.05$, 70 mW/cm^2 versus control. $^{**}P < 0.01$, $^{***}P < 0.001$ 140 mW/cm^2 versus control. $\#P < 0.01$, $\#\#\#P < 0.001$, 210 mW/cm^2 versus control, one-way ANOVA. B. Proliferation was quantified by EdU assay. Scale bar = 50 μm. C. Quantification of EdU staining showed that 140 and 210 mW/cm^2 LIPUS doses decreased the number of EdU-positive cells (proliferation) compared with control treatment. Data are mean ± SEM. ns $P > 0.05$, $^{***}P < 0.001$ versus control, one-way ANOVA.

(**Figure 1D**). However, increased cell viability was seen with an ultrasound intensity of 70 mW/cm^2, while the 210 mW/cm^2 dose decreased cell viability (**Figure 1D**), similar to the

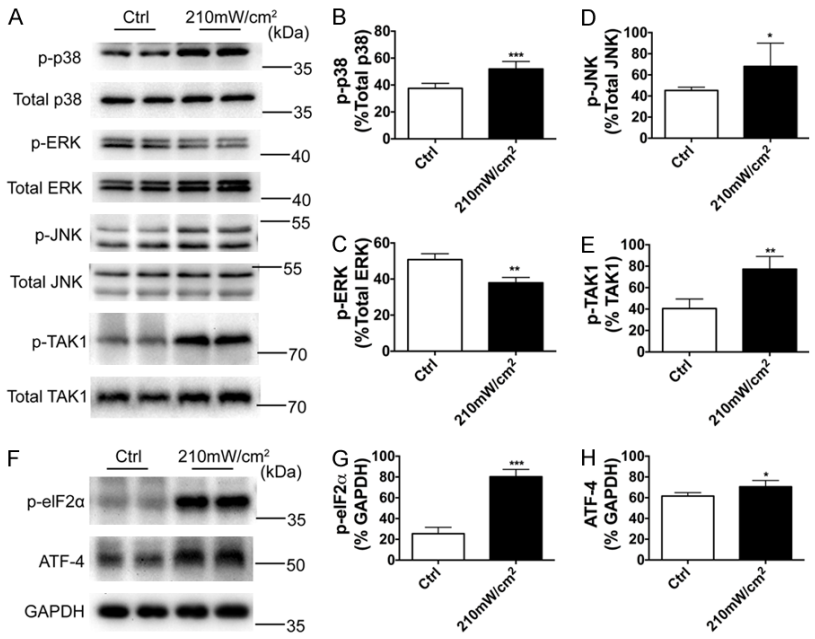

Figure 3. High dose of LIPUS promotes apoptosis via phosphorylation of p38. A. Western blot analysis of p-p38, total p38, p-ERK, total ERK, p-JNK, total JNK, p-TAK1 and total TAK1 expression in hAMSCs treated with an ultrasound intensity of 210 mW/cm^2. B. Quantification of p-p38 levels relative to total p38. Data are mean ± SEM. ***P < 0.001 versus control, unpaired t-test. C. Quantification of p-ERK levels relative to total ERK. Data are mean ± SEM. **P < 0.01 versus control, unpaired t-test. D. Quantification of p-JNK levels relative to total JNK. Data are mean ± SEM. *P < 0.05 versus control, unpaired t-test. E. Quantification of p-TAK1 levels relative to total TAK1. Data are mean ± SEM. **P < 0.01 versus control, unpaired t-test. F. Western blot analysis of p-eIF2α, ATF-4 and GAPDH expression in hAMSCs treated with an ultrasound intensity of 210 mW/cm^2. G. Quantification of p-eIF2α levels relative to GAPDH. Data are mean ± SEM. ***P < 0.001 versus control, unpaired t-test. H. Quantification of ATF-4 levels relative to GAPDH. Data are mean ± SEM. *P < 0.05 versus control, unpaired t-test.

results shown in **Figure 1C**. We performed real-time cell analysis (RTCA) of LIPUS-treated synchronized hAMSCs to study differences in cell proliferation rates under different ultrasound intensities. We found no significant differences in proliferation rates between control cells and cells treated with an ultrasound intensity of 70 mW/cm^2 (**Figure 2A**). Furthermore, ultrasound intensities of 140 mW/cm^2 and 210 mW/cm^2 significantly inhibited cell proliferation compared with the control treatment (**Figure 2A**). To further confirm the effect of LIPUS on cell proliferation, the cells were then incubated with EdU to label DNA synthesis and cell proliferation. As expected, the 70 mW/cm^2 dose of LIPUS did not affect cell proliferation, but 140 mW/cm^2 and 210 mW/cm^2 LIPUS doses decreased cell proliferation (**Figure 2B** and **2C**). Our results indicated that a low dose LIPUS treatment enhanced cell viability but not proliferation in hAMSCs, while high dose LIPUS treatment inhibited cell viability and proliferation.

Dose-dependent opposing effects of LIPUS on cell viability are mediated by p38 phosphorylation

Our previous study showed that a specific intensity of LIPUS (109.44 mW/cm^2) promoted cell apoptosis via the p38 MAPK pathway [22]. To test if the apoptotic effects of high dose LIPUS treatment on hAMSCs were also mediated by the p38 pathway, we measured levels of MAPK pathway proteins in cells treated with an ultrasound intensity of 210 mW/cm^2. LIPUS treatment increased the levels of phosphorylated p38 and JNK, and decreased the level of the p-ERK (**Figure 3A-D**). Furthermore, LIPUS treatment increased the level of p-TAK1, which regulates p38 activation in cell apoptosis (**Figure 3A** and **3E**). To determine the downstream targets of p38 in LIPUS induced cell apoptosis, we also quantified p-eIF2α, the key protein involved in endoplasmic stress, and its downstream effector ATF-4. We found that LIPUS treatment significantly increased the levels of both p-eIF2α and ATF-4 (**Figure 3F-H**). We then examined whether p38 modulated this signaling transduction from TAK1 to p-eIF2α via p38 inhibition. Importantly exposure of high dose LIPUS-treated hAMSCs to the p38 inhibitor, SB203580, significantly decreased cell apoptosis (**Figure 4A**, **4B**). Furthermore, p38 inhibition (**Figure 4C**) significantly attenuated the LIPUS-enhanced expression of p-TAK1 and p-eIF2α, but not ATF-4 (**Figure 4D-F**). In contrast, LIPUS stimulation of hAMSCs with an intensity of 70 mW/cm^2 significantly decreased the levels of p-p38 and increased the levels of p-ERK (**Figure 5A-C**). A slight elevation in the

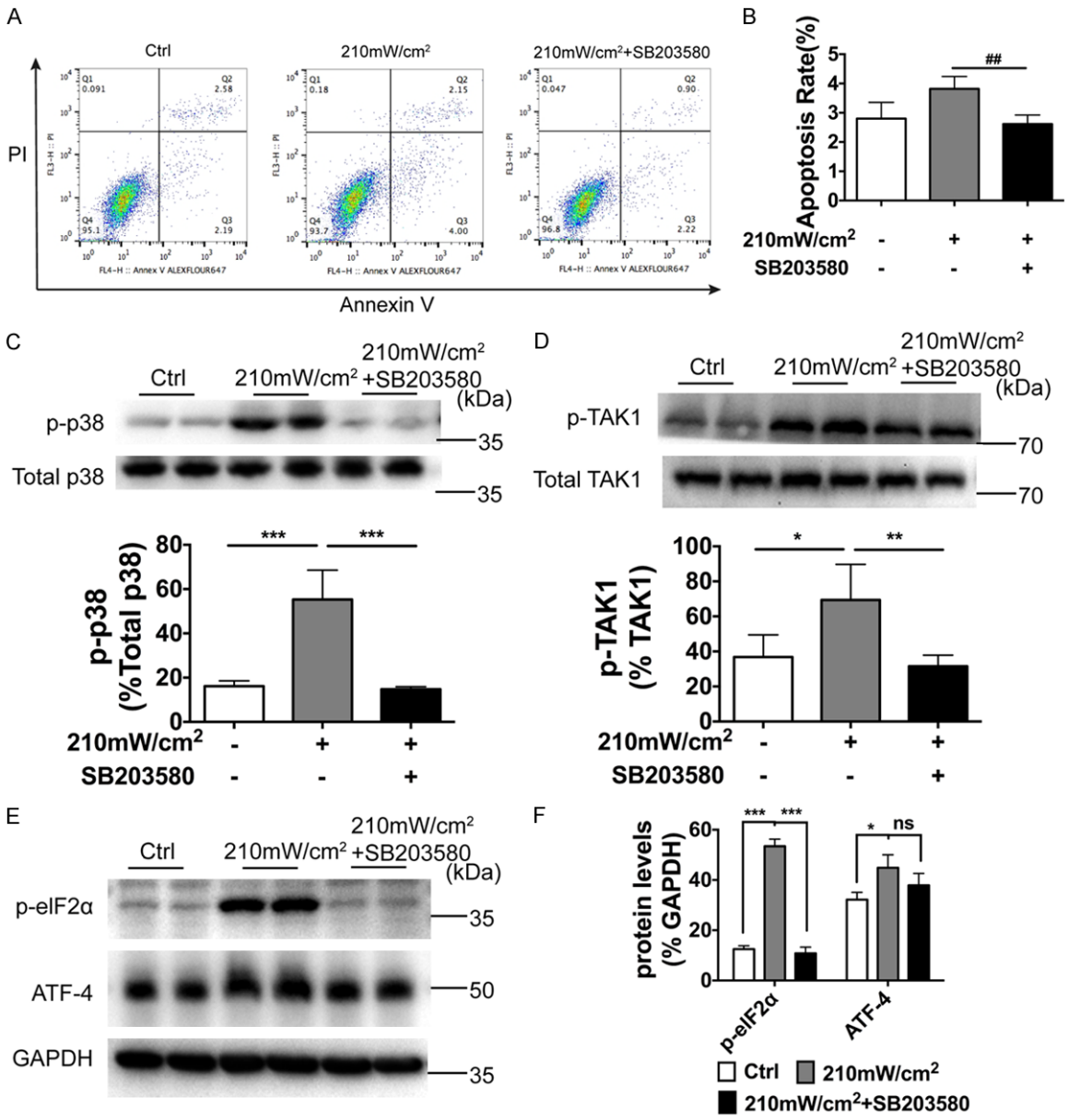

Figure 4. Inhibition of p38 abolishes LIPUS-induced cell apoptosis. A. Flow cytometric analysis of apoptosis rates in hAMSCs at an ultrasound intensity of 210 mW/cm^2 and treated with the MAPK p38 inhibitor, SB203580 (2 mM), for 24 h. The lower right quadrant shows early apoptotic cells. B. Apoptosis rate of hAMSCs 24 h after LIPUS treatment and treatment with the MAPK p38 inhibitor, SB203580 (2 mM). Data are mean ± SEM. ## $P < 0.01$ versus 210 mW/cm^2, one-way ANOVA. C. Western blot analysis of p-p38 and p38. Quantification of p-p38 levels relative to total p38. p38 inhibition by SB203580 was verified. Data are mean ± SEM. ***$P < 0.001$, one-way ANOVA. D. Western blot analysis of p-TAK1 and total TAK1. Quantification of p-TAK1 levels relative to total TAK1. p38 inhibition slightly reversed the enhanced expression of p-TAK1. Data are mean ± SEM. *$P < 0.05$, **$P < 0.01$. one-way ANOVA. E. Western blot analysis of p-eIF2α, ATF-4, and GAPDH expression in hAMSCs treated with SB203580 after treatment with an ultrasound intensity of 210 mW/cm^2. F. Quantification of the indicated proteins relative to GAPDH. Data are mean ± SEM. ns $P > 0.05$, *$P < 0.05$, ***$P < 0.001$, one-way ANOVA.

levels of p-JNK was also observed (**Figure 5A** and **5D**). Our results showed that the dose-dependent LIPUS-mediated effects on cell apoptosis occurred via the p38/MAPK-mediated signaling pathway.

Discussion

Visceral obesity is a major reason for serious health complications such as diabetes and cardiovascular disease [3]. It has been shown that

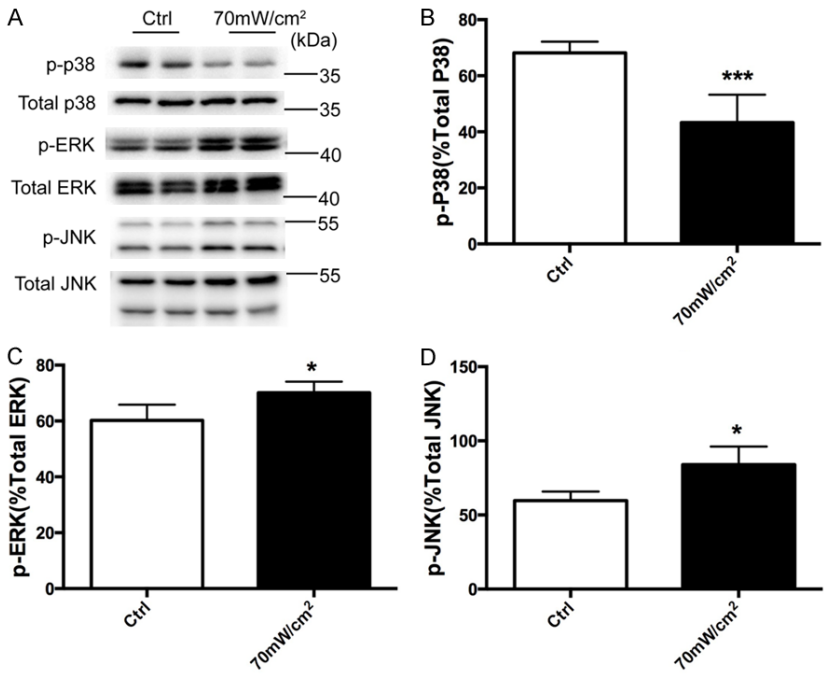

Figure 5. Low dose of LIPUS decreases phosphorylation of p38. A. Western blot analysis of p-p38, total p38, p-ERK, total ERK, p-JNK, and total JNK expression in hAMSCs treated with an ultrasound intensity of 70 mW/cm^2. B. Quantification of p-p38 levels relative to total p38. Data are mean ± SEM. ***P < 0.001 versus control, unpaired t-test. C. Quantification of p-ERK levels relative to total ERK. Data are mean ± SEM. *P < 0.05 versus control, unpaired t-test. D. Quantification of p-JNK levels relative to total JNK. Data are mean ± SEM. *P < 0.05 versus control, unpaired t-test.

500 cm^3 of visceral adipose tissue above baseline levels results in a 1.3-fold increase in the risk of developing hypertension and a 2.58-fold increase in the risk of developing metabolic syndrome in women [1, 2]. Omentectomy prevents metabolic syndrome by reducing appetite and body weight in diet-induced obesity rat models [8]. The widespread global prevalence of obesity and its associated health issues require the need for urgent therapeutic measures. Bariatric surgery is one option to treat severe obesity, but its invasive approach limits its clinical applications. The use of medications for reducing obesity carries risks of side effects. Lifestyle modification is the safest way to tackle obesity. However, a long-term commitment to exercise and diet control is challenging for many people. Also, some patients fail to respond to lifestyle changes because of certain pre-existing genetic disorders [25]. Therefore, an alternative means of therapy is necessary for the control of visceral obesity.

Adipose tissue contains a population of mesenchymal stem cells (MSCs) located in the stromal vascular fraction [26, 27]. The adipogenic differentiation ability of MSCs enables them to spontaneously repair adipose tissue after injury. The removal of adipose tissue (such as liposuction) is not a long-term remedy for obesity because it results in a compensatory increase in visceral adipose tissue [28]. The removal of fat tissue likely sends a false signal to MSCs to activate this repair mechanism. Obesity also results in impaired MSC function and remodeling of adipose tissue, which worsens the condition [29]. Treatments targeting adipose MSCs may provide a potential therapeutic strategy for visceral obesity.

LIPUS is emerging as a safe and non-invasive therapy for treating non-union fractures [30]. Several studies have shown that LIPUS improves endothelial function [25] and protects against endothelial-mesenchymal transition [31] and spinal fusion [17]. LIPUS has also been reported to alter cell apoptosis, viability and proliferation [13-16]. Several studies have reported that LIPUS influences differentiation of adipose-derived stem cells [18-20]. It is clear that the mechanical effects of LIPUS are translated into various cellular effects. The cellular effects of LIPUS on adipose-derived MSCs have not been previously studied. Here, we showed that different intensities of LIPUS induced specific cellular effects in hAMSCs. We also explored its potential therapeutic value in obesity control.

We found that a high dose of LIPUS (210 mW/cm^2) promoted apoptosis in hAMSCs, while a low dose (70 mW/cm^2) enhanced cell viability without affecting proliferation. Phosphorylation of p38 significantly increased in cells treated with high dose LIPUS, but dramatically decreased in low dose-treated cells. Meanwhile, LIPUS also increased the levels of p-TAK1,

which activates p38 during stress-induced cell apoptosis. These data suggest that a high dose of LIPUS promoted cell apoptosis via activation of the TAK1-p38 axis. Alternatively, high dose LIPUS also increased the expression of p-eIF2α and its downstream effector ATF-4. These results revealed that LIPUS-induced cell apoptosis involves endoplasmic reticulum stress. Furthermore, our data showed that inhibition of p38 phosphorylation by SB203580 rescued both the apoptotic effects of LIPUS and the associated changes in protein levels of p-eIF2α, but not ATF4. This suggests that LIPUS-induced endoplasmic reticulum stress is partially p-p38 dependent. Interestingly, p38 inhibition did not affect LIPUS-induced ATF-4 expression, indicating that there is some endogenous compensation. Our findings indicate that the p38 MAPK pathway plays a key role in mediating the differential effects of LIPUS on hAMSCs.

In our previous study [22], LIPUS-treated rat primary visceral preadipocytes showed increased rates of apoptosis at a dosage intensity of 109.44 mW/cm^2. In this study, a dosage intensity of 140 mW/cm^2 was not sufficient to induce apoptosis in hAMSCs. Increased rates of apoptosis were only observed when hAMSCs were treated with LIPUS at a high dosage intensity of 210 mW/cm^2. These results suggest that hAMSCs needed larger amounts of ultrasound energy to undergo cellular apoptosis compared with rat primary visceral preadipocytes. The difference in species and cellular origins of the two cell types analyzed in the two studies may contribute to their different energy requirements to undergo apoptosis. The primary visceral adipocytes from rats used in our previous study were derived from epididymal adipose tissue [22], while the hAMSCs used in the current study were derived from human omental adipose tissue. Omental adipose tissue acts as a shock absorber that provides padding to protect inner organs from physical injury. This type of adipose tissue is enriched in fibrillar proteins compared with subcutaneous adipose tissue, which contributes to its mechanical properties [32]. Subcutaneous adipose tissue has a lower energy dissipation density and slower stress relaxation properties than omental adipose tissue, which suggests that these two tissue types have different biomechanical properties [32]. Our results reflected these differences in tissue types derived from rat and human cells. Thus LIPUS parameters obtained from animal studies may not be extrapolated to human cells. The clinical development of LIPUS therapy for abdominal obesity requires better analysis of effective ultrasound parameters.

It has been shown that a low dose of LIPUS treatment, but not a high dose, enhances fracture healing [11, 33]. Low-density bone volume fractions and woven bone percentages were compared between cells treated with 30 mW/cm^2 and 150 mW/cm^2 doses of LIPUS. Cells that were treated with an ultrasound dose intensity of 30 mW/cm^2 showed significantly enhanced fracture healing compared with cells treated with an ultrasound dose intensity of 150 mW/cm^2 [27]. A low dose of LIPUS (30 mW/cm^2) has been shown to suppress adipogenic differentiation and promote osteogenic differentiation in 3T3-L1 and ST2 cell lines by inducing ERK phosphorylation [28]. In contrast, a high dose of LIPUS (100 mW/cm^2) promotes adipogenic differentiation of adipose-derived stem cells in mice [29]. These studies suggest a key role for ERK phosphorylation in adipogenic differentiation of AMSCs. In our study, we showed that different doses of LIPUS had different cellular effects on hAMSCs. Specifically, a high dose of LIPUS (210 mW/cm^2) promoted apoptosis, while a low dose (70 mW/cm^2) enhanced cell viability. ERK phosphorylation was increased in cells treated with a high dose of LIPUS, but decreased in cells treated with a low dose. It is possible that ERK phosphorylation is also involved in adipogenic differentiation of hAMSCs; however, further studies are needed to test this premise.

To determine the main force in LIPUS treatment, we tested temperature upon 70-210 mW/cm^2 doses of LIPUS and found that upon 70 mW/cm^2, the temperature reached 30°C, while upon 140 and 210 mW/cm^2, the temperature reached 35°C. Because the 210 mW/cm^2 dose of LIPUS promoted cell apoptosis, while 140 mW/cm^2 did not, we speculate that the pro-apoptotic effects of LIPUS may be caused by the mechanical rather than thermal changes.

In summary, we found that a high dose of LIPUS (210 mW/cm^2) promoted apoptosis, while a low dose (70 mW/cm^2) enhanced cell viability in hAMSCs. Phosphorylation of p38 was a potential key mechanism mediating the differential effects of LIPUS. Further *in vivo* studies are

needed to determine the optimal doses of ultrasound intensities that reduce visceral adipose volume without causing side effects. Our study showed the potential use of LIPUS as a safe and non-invasive therapy to control visceral obesity and attenuate related health complications.

Acknowledgements

This work was supported by grants from the National Natural Science Foundation of China (No. 81627802, No. 81570247) and the Priority Academic Program Development of Jiangsu Higher Education Institutions (PAPD2014-2016). Dr. Wei Sun is an assistant Fellow at the Collaborative Innovation Center for Cardiovascular Disease Translational Medicine, Dr. Xiangqing Kong is a Fellow at the Collaborative Innovation Center for Cardiovascular Disease Translational Medicine.

Disclosure of conflict of interest

None.

Address correspondence to: Wei Sun and Xiangqing Kong, Department of Cardiology, The First Affiliated Hospital of Nanjing Medical University, 300 Guangzhou Road, Nanjing 210029, PR China. Tel: 86 25 68135272; Fax: 86 25 84352775; E-mail: weisun7919@njmu.edu.cn (WS); Kongxq_njmu@outlook.com (XQK)

References

[1] Abraham TM, Pedley A, Massaro JM, Hoffmann U and Fox CS. Association between visceral and subcutaneous adipose depots and incident cardiovascular disease risk factors. Circulation 2015; 132: 1639-1647.

[2] Lee JJ, Pedley A, Hoffmann U, Massaro JM and Fox CS. Association of changes in abdominal fat quantity and quality with incident cardiovascular disease risk factors. J Am Coll Cardiol 2016; 68: 1509-1521.

[3] Nigro E, Scudiero O, Monaco ML, Palmieri A, Mazzarella G, Costagliola C, Bianco A and Daniele A. New insight into adiponectin role in obesity and obesity-related diseases. Biomed Res Int 2014; 2014: 658913.

[4] Janssen I, Katzmarzyk PT and Ross R. Waist circumference and not body mass index explains obesity-related health risk. Am J Clin Nutr 2004; 79: 379-384.

[5] Kanaya AM, Vittinghoff E, Shlipak MG, Resnick HE, Visser M, Grady D and Barrett-Connor E. Association of total and central obesity with mortality in postmenopausal women with coronary heart disease. Am J Epidemiol 2003; 158: 1161-1170.

[6] Fukuhara A, Matsuda M, Nishizawa M, Segawa K, Tanaka M, Kishimoto K, Matsuki Y, Murakami M, Ichisaka T, Murakami H, Watanabe E, Takagi T, Akiyoshi M, Ohtsubo T, Kihara S, Yamashita S, Makishima M, Funahashi T, Yamanaka S, Hiramatsu R, Matsuzawa Y and Shimomura I. Visfatin: a protein secreted by visceral fat that mimics the effects of insulin. Science 2005; 307: 426-430.

[7] Srivastava G and Apovian CM. Current pharmacotherapy for obesity. Nat Rev Endocrinol 2018; 14: 12-24.

[8] Garcia-Ruiz I, Solis-Munoz P, Fernandez-Moreira D, Grau M, Munoz-Yague MT and Solis-Herruzo JA. Omentectomy prevents metabolic syndrome by reducing appetite and body weight in a diet-induced obesity rat model. Sci Rep 2018; 8: 1540.

[9] Lehmann JF. The biophysical basis of biologic ultrasonic reactions with special reference to ultrasonic therapy. Arch Phys Med Rehabil 1953; 34: 139-152.

[10] Nolte P, Anderson R, Strauss E, Wang Z, Hu L, Xu Z and Steen RG. Heal rate of metatarsal fractures: a propensity-matching study of patients treated with low-intensity pulsed ultrasound (LIPUS) vs. surgical and other treatments. Injury 2016; 47: 2584-2590.

[11] Harrison A, Lin S, Pounder N and Mikuni-Takagaki Y. Mode & mechanism of low intensity pulsed ultrasound (LIPUS) in fracture repair. Ultrasonics 2016; 70: 45-52.

[12] Zura R, Della Rocca GJ, Mehta S, Harrison A, Brodie C, Jones J and Steen RG. Treatment of chronic (>1 year) fracture nonunion: heal rate in a cohort of 767 patients treated with low-intensity pulsed ultrasound (LIPUS). Injury 2015; 46: 2036-2041.

[13] Shi M, Liu B, Liu G, Wang P, Yang M, Li Y and Zhou J. Low intensity-pulsed ultrasound induced apoptosis of human hepatocellular carcinoma cells in vitro. Ultrasonics 2016; 64: 43-53.

[14] Suzuki N, Hanmoto T, Yano S, Furusawa Y, Ikegame M, Tabuchi Y, Kondo T, Kitamura K, Endo M, Yamamoto T, Sekiguchi T, Urata M, Mikuni-Takagaki Y and Hattori A. Low-intensity pulsed ultrasound induces apoptosis in osteoclasts: fish scales are a suitable model for the analysis of bone metabolism by ultrasound. Comp Biochem Physiol A Mol Integr Physiol 2016; 195: 26-31.

[15] Matsuo T, Sato K, Matsui T, Sawada S, Muramatsu Y, Kawanami K and Deie M. Inhibitory effects of low-intensity pulsed ultrasound sonication on the proliferation of osteosarcoma cells. Oncol Lett 2017; 14: 3071-3076.

[16] Ren C, Chen X, Du N, Geng S, Hu Y, Liu X, Wu X, Lin Y, Bai X, Yin W, Cheng S, Yang L and Zhang Y. Low-intensity pulsed ultrasound promotes Schwann cell viability and proliferation via the GSK-3beta/beta-catenin signaling pathway. Int J Biol Sci 2018; 14: 497-507.

[17] Zhou XY, Xu XM, Wu SY, Zhang ZC, Wang F, Yang YL, Li M and Wei XZ. Low-intensity pulsed ultrasound promotes spinal fusion and enhances migration and proliferation of MG63s through sonic hedgehog signaling pathway. Bone 2018; 110: 47-57.

[18] Zhang Z, Ma Y, Guo S, He Y, Bai G and Zhang W. Low-intensity pulsed ultrasound stimulation facilitates in vitro osteogenic differentiation of human adipose-derived stem cells via up-regulation of heat shock protein (HSP)70, HSP90, and bone morphogenetic protein (BMP) signaling pathway. Biosci Rep 2018; 38.

[19] Uddin SM and Qin YX. Enhancement of osteogenic differentiation and proliferation in human mesenchymal stem cells by a modified low intensity ultrasound stimulation under simulated microgravity. PLoS One 2013; 8: e73914.

[20] Fu N, Yang X, Ba K, Fu Y, Wei X, Yue Y, Li G, Yao Y, Chen J, Cai X, Liang C, Ge Y and Lin Y. Low-intensity pulsed ultrasound induced enhanced adipogenesis of adipose-derived stem cells. Cell Prolif 2013; 46: 312-319.

[21] Kim JS, Lee DJ, Lee YS and Lee BK. A study of abdominal ultrasound therapy combined with complex exercise for effective obesity management among shift work employees. J Phys Ther Sci 2015; 27: 231-233.

[22] Xu T, Gu J, Li C, Guo X, Tu J, Zhang D, Sun W and Kong X. Low-intensity pulsed ultrasound suppresses proliferation and promotes apoptosis via p38 MAPK signaling in rat visceral preadipocytes. Am J Transl Res 2018; 10: 948-956.

[23] Aurich H, Sgodda M, Kaltwasser P, Vetter M, Weise A, Liehr T, Brulport M, Hengstler JG, Dollinger MM, Fleig WE and Christ B. Hepatocyte differentiation of mesenchymal stem cells from human adipose tissue in vitro promotes hepatic integration in vivo. Gut 2009; 58: 570-581.

[24] McArthur K and Kile BT. Apoptotic Caspases: Multiple or Mistaken Identities? Trends Cell Biol 2018; 28: 475-493.

[25] Montague CT, Farooqi IS, Whitehead JP, Soos MA, Rau H, Wareham NJ, Sewter CP, Digby JE, Mohammed SN, Hurst JA, Cheetham CH, Earley AR, Barnett AH, Prins JB and O'Rahilly S. Congenital leptin deficiency is associated with severe early-onset obesity in humans. Nature 1997; 387: 903-908.

[26] Louwen F, Ritter A, Kreis NN and Yuan J. Insight into the development of obesity: functional alterations of adipose-derived mesenchymal stem cells. Obes Rev 2018; 19: 888-904.

[27] Bauer-Kreisel P, Goepferich A and Blunk T. Cell-delivery therapeutics for adipose tissue regeneration. Adv Drug Deliv Rev 2010; 62: 798-813.

[28] Benatti F, Solis M, Artioli G, Montag E, Painelli V, Saito F, Baptista L, Costa LA, Neves R, Seelaender M, Ferriolli E, Pfrimer K, Lima F, Roschel H, Gualano B and Lancha A Jr. Liposuction induces a compensatory increase of visceral fat which is effectively counteracted by physical activity: a randomized trial. J Clin Endocrinol Metab 2012; 97: 2388-2395.

[29] Badimon L and Cubedo J. Adipose tissue depots and inflammation: effects on plasticity and resident mesenchymal stem cell function. Cardiovasc Res 2017; 113: 1064-1073.

[30] Wang Y, Newman MR and Benoit DSW. Development of controlled drug delivery systems for bone fracture-targeted therapeutic delivery: A review. Eur J Pharm Biopharm 2018; 127: 223-236.

[31] Li J, Zhang Q, Ren C, Wu X, Zhang Y, Bai X, Lin Y, Li M, Fu J, Kopylov P, Wang S, Yu T, Wang N, Xu C and Yang B. Low-intensity pulsed ultrasound prevents the oxidative stress induced endothelial-mesenchymal transition in human aortic endothelial cells. Cell Physiol Biochem 2018; 45: 1350-1365.

[32] Alkhouli N, Mansfield J, Green E, Bell J, Knight B, Liversedge N, Tham JC, Welbourn R, Shore AC, Kos K and Winlove CP. The mechanical properties of human adipose tissues and their relationships to the structure and composition of the extracellular matrix. Am J Physiol Endocrinol Metab 2013; 305: E1427-1435.

[33] Fung CH, Cheung WH, Pounder NM, de Ana FJ, Harrison A and Leung KS. Effects of different therapeutic ultrasound intensities on fracture healing in rats. Ultrasound Med Biol 2012; 38: 745-752.

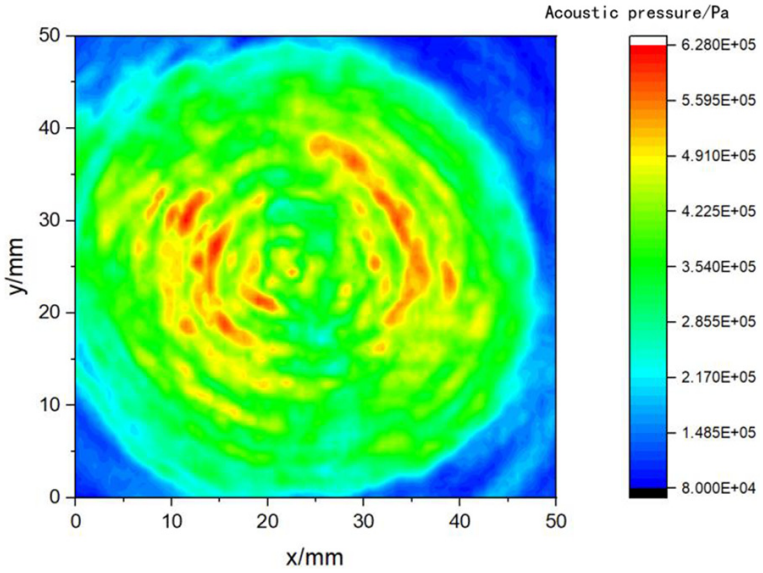

Supplementary Figure 1. Acoustic pressure in this study.

Supplementary Table 1. List of acoustic parameters used in this study

Frequency (MHz)	Number of cycles	Ultrasonic power (W)	Ultrasound intensity (mW/cm^2)	Temperature (°C)
0.5	1,000	1.42	70	30
	2,000	2.80	140	35
	3,000	4.16	210	35

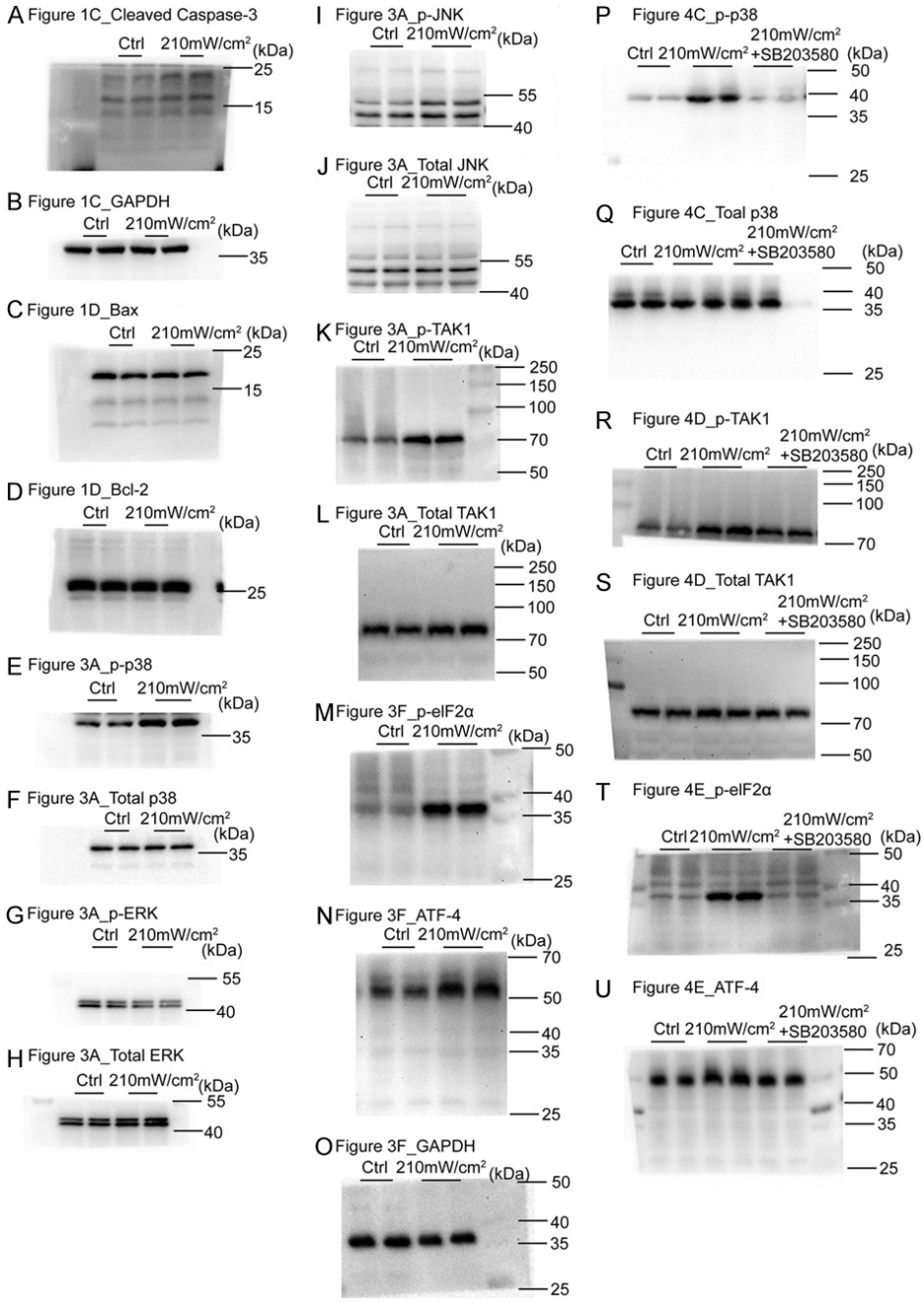

Supplementary Figure 2. Original western images for all relevant western blots.

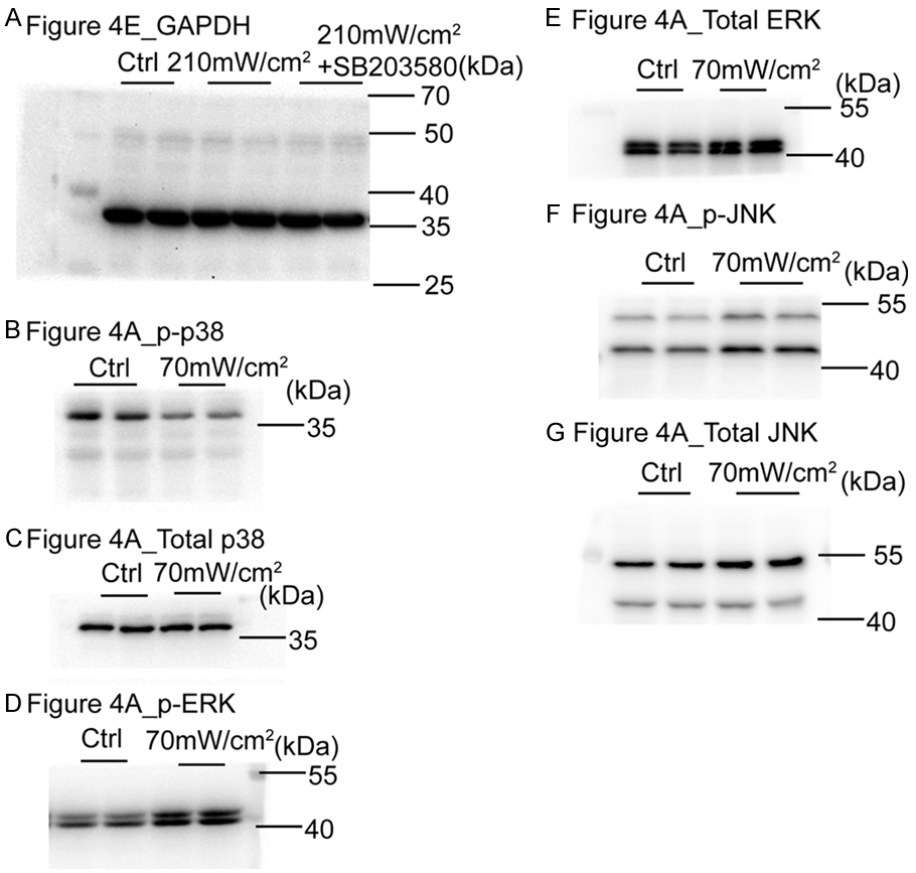

Supplementary Figure 3. Original western images for all relevant western blots.